



Original research article

Production of graphene powder by electrochemical exfoliation of graphite electrodes immersed in aqueous solution



Raneen Imad Jibrael, Mustafa K.A. Mohammed*

Department of Applied Science, University of Technology, Baghdad, Iraq

ARTICLE INFO

Article history:

Received 28 February 2016

Accepted 19 April 2016

Keywords:

Graphene

Electrochemical exfoliation

Raman spectroscopy

Aqueous solution

Graphite electrodes

ABSTRACT

In our research, graphene powder was prepared by electrochemical exfoliation of graphite electrodes immersed in electrolyte solution of a sulfuric acid, nitric acid and distilled water ($\text{H}_2\text{SO}_4/\text{HNO}_3/\text{H}_2\text{O}$) with applied +10V for 50 min. Graphene powder was characterized by XRD, Raman spectroscopy, AFM, SEM, and FTIR to investigate the structural, morphological, and chemical properties. The XRD analysis was showed polycrystalline structure of graphene with sharp peak at $2\theta=26.61$ and broad peak at $2\theta=54.68$ along (002) and (004) orientation respectively which was consistent with the interlayer spacing of normal graphite. Raman spectrum was demonstrated two intensive peaks at 1580 cm^{-1} and 1354 cm^{-1} for I_G and I_D confirmed with graphitic carbon-based materials. The AFM and SEM were exhibited the morphology of graphene powder has different shapes and sizes with a few agglomerates of crumpled and rippled structure. FTIR spectrum showed an absorption band at 1643.41 cm^{-1} assigned to the C=C stretching vibration of the hexagonal ring also there were oxygen-containing functional groups such as C–O and O–H.

© 2016 Elsevier GmbH. All rights reserved.

1. Introduction

Graphene is a two-dimensional (2D) layer of carbon atoms ordered into a hexagonal structure called honeycomb lattice [1]. Graphene, one of the allotropes (carbon nanotube, fullerene, diamond) of elemental carbon [2], is a planar monolayer of carbon atoms with a carbon–carbon bond length of 0.142 nm [3]. Graphene exhibits superior electrical conductivity and a high charge carrier mobility ($20\text{ m}^2\text{ V}^{-1}\text{ s}^{-1}$) [4] because electron tunneling occurs within its structure allowing electron movement at relativistic speeds. It has been reported to have the fastest electron and hole mobility than any other material [5]. It also has a high specific surface area ($2630\text{ m}^2\text{ g}^{-1}$), which could be likened to that of a soccer pitch per gram [6], excellent mechanical strength and stiffness, good elasticity, superior thermal conductivity, a broad electrochemical window and can offer as optical transparency [7]. A particularly promising graphene production technique is based on the obtainment of colloidal suspensions from graphite, or its derivatives [8]. In spite of other methods like epitaxial growth, chemical vapor deposition, and micromechanical exfoliation, this approach is both scalable, affording the possibility of high-volume production, and versatile in terms of chemical functionalization, which, on the other hand, is sometimes exploited to favor graphene obtainment and its dispersion [9]. The electrochemical approach has the advantages of being single-step, easy to operate, environmentally friendly (if using ionic liquid electrolytes or aqueous surfactants) and operates at ambient

* Corresponding author.

E-mail address: Mustafa_kareem97@yahoo.com (M.K.A. Mohammed).

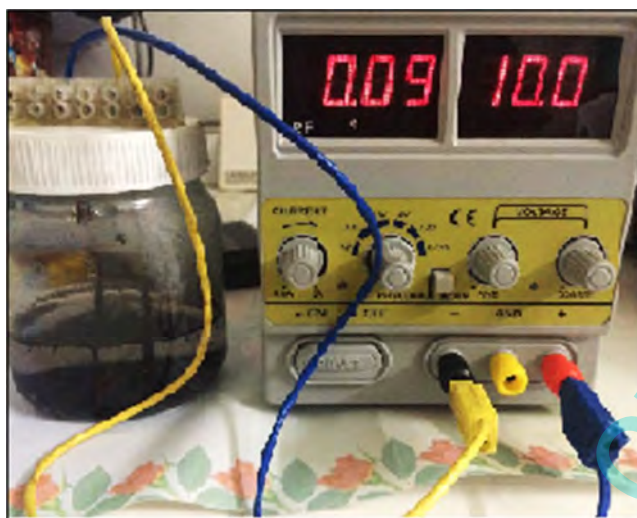


Fig. 1. Experimental setup of electrochemical exfoliation technique.

conditions [10]. Highly controllable flakes can be formed without the need for volatile solvents or reducing agents. The process can take several minutes to hours to complete and the reported results are encouraging for the fast-processing of large quantities of graphene flakes [11]. The electrochemical method utilizes a liquid solution (electrolyte) and an electrical current to drive structural expansion (oxidation or reduction), intercalation and exfoliation at a piece of graphite (rod, plate, wire) to produce graphene flakes. The experimental arrangement uses a monopolar, undivided electrolysis cell. The yield, productivity and properties of graphene flakes can be tuned by controlling the electrolysis parameters and electrolytes [12]. In this paper we attempted to prepare graphene by using graphite (pencil) as anode and cathode electrodes and immersed into the electrolyte solution (HNO_3 , H_2SO_4 and H_2O), which will act as intercalate and studying the structural, morphological, and chemical properties.

2. Experimental details

Electrochemical exfoliation was carried out in an electrolysis cell shown as Fig. 1. This cell has graphite electrodes (pencil) as anode and as cathode and the separation distance between graphite electrodes was fixed at 4 cm shown as Fig. 2(a). These electrodes were immersed in electrolyte solution of sulfuric acid H_2SO_4 (0.69 gm) and nitric acid HNO_3 (0.19 gm) dissolved to 1000 ml of de-ionized water to make pH solution value around 3 at room temperature. The electrochemical exfoliation was done by first applying DC voltage of +1 V for 5 min and then we increased the voltages for 5 min +1 V until reached +10 V at 50 min. The application of high voltages on the anode resulted in the gradual exfoliation of graphite through edges. Afterwards, the graphene foam was extracted from electrolysis cell demonstrated in Fig. 2(d) and dried by using vacuum oven at 200°C for two hours.

3. Material characterization

Structural properties were performed by X-ray Diffraction (XRD) according to the Joint Committee on Powder Diffraction Standards (JCPDS) card, using Shimadzu XRD-7000 X-ray diffractometer using $\text{CuK}\alpha$ ($\lambda = 1.54050 \text{ \AA}$) irradiation operated at 40 kV and 30 mA and by Raman spectrometer (Senterra Raman microscope Bruker co., Germany), which is double monochromatic instrument use a green laser ($\lambda = 532 \text{ nm}$) as an excitation source. Morphological properties were characterized by scanning electron microscopy (SEM) (The VEGA Easy Probe) and atomic force microscopy (AFM) using a scanning probe microscopy (CSPM-5000) instrument. Chemical properties measured by Fourier transform infrared (FTIR) spectra with KBr disc were recorded using: FT-IR-8400S Shimadzu in the range of $400\text{--}4000 \text{ cm}^{-1}$ at room temperature.

4. Results and discussion

4.1. Structural properties

Fig. 3 shows the XRD pattern of graphene powder prepared by electrochemical exfoliation method, the XRD exhibited the structure of graphene is polycrystalline has two peaks, a strong sharp diffraction peak at $2\theta = 26.61^\circ$, corresponds to an interlayer distance of 3.346°A for (002) which is consistent with the interlayer spacing of normal graphite according to JCPDS card (230064), which has interlayer distance equal to 3.35°A and a weak and broad diffraction peak at 54.68° of 2θ

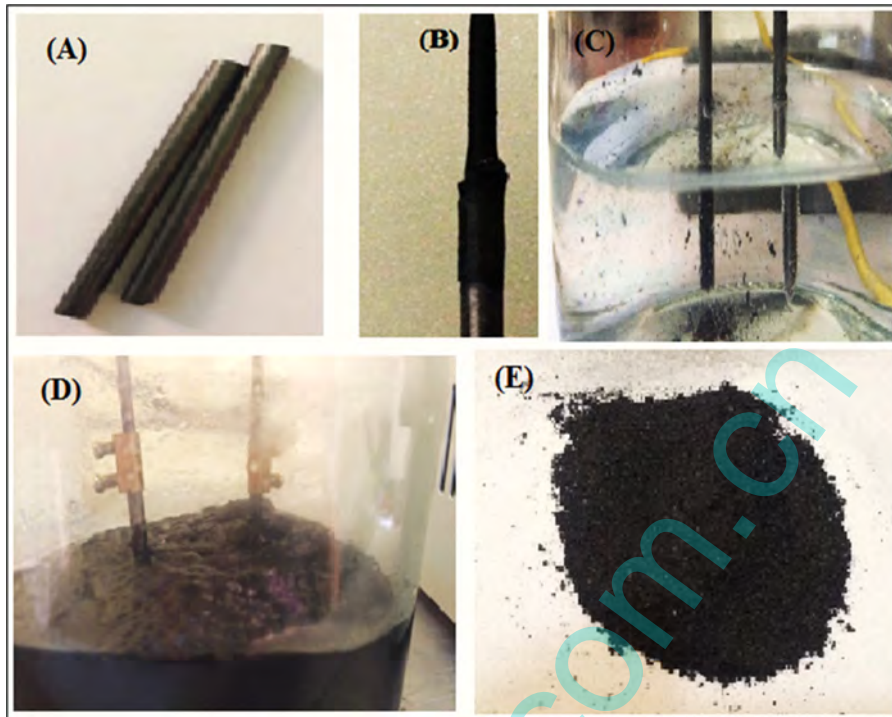


Fig. 2. (a) Photo of graphite electrodes before exfoliation and (b) after exfoliation process. (c) photo of the dispersed graphene sheets in aqueous solution after applying +2 V for 10 min and (d) after applying +10 V for 50 min e) dried graphene powder.

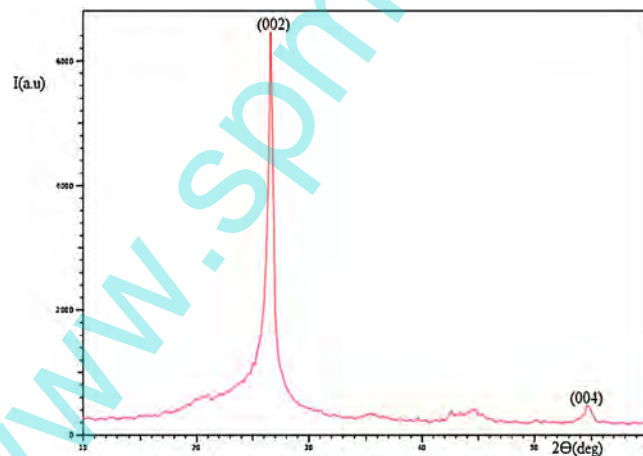


Fig. 3. XRD pattern of graphene powder.

corresponding to the interlayer distance of 1.67 \AA along the (004) orientation. The crystallite size of graphene has been measured by applying the full width half maximum (FWHM) of the peak into Eq. (1) [13].

$$L = \frac{k\lambda}{B\cos\theta} \quad (\text{Scherrer Eq.}) \quad (1)$$

where L is crystallite size (nm) equal to 11.85 nm, B is FWHM and k is a constant ($k=0.89$). Furthermore, the strain ($\varepsilon\%$) of the nanocrystalline graphene along the c-axis can be calculated using the following Eq.:

$$\text{Micros strain } (\varepsilon\%) = \frac{c - c_0}{c_0} \quad (2)$$

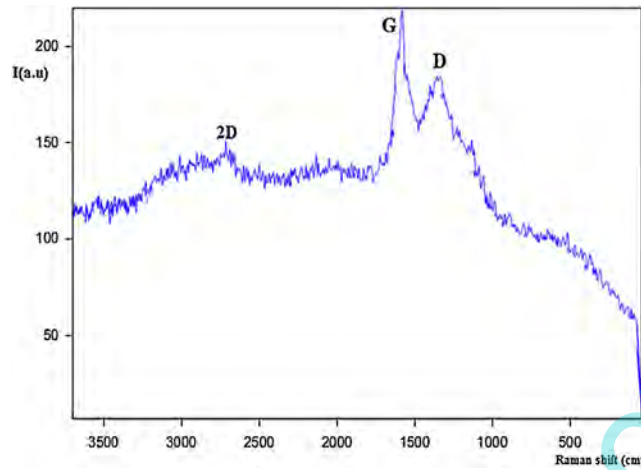


Fig. 4. Raman spectrum of graphene.

where c is the lattice constant of the strained graphene calculated from XRD data by using Eq. (3) equal to 6.692 \AA and c_0 is the unstrained lattice constant for hexagonal graphite are reported in JCPDS standard data $c_0 = 6.72 \text{ \AA}$

$$\frac{1}{d^2} = \frac{4}{3} \times \left(\frac{h^2 + hk + k^2}{a^2} \right) + \frac{l^2}{c^2} \quad (3)$$

The obtained value of strain was -0.0041 for (002). A negative value is associated with compression strain. The low value of the compression strain revealed that the graphene referred to grow along the c -axis, and gave evidence of a high-quality crystal resulting.

Raman spectroscopy is a non-destructive technique that is widely used to obtain structural information about carbon-based materials [14]. Raman spectrum of graphene obtained at an excitation wavelength of 532 nm is shown in Fig. 4. The main features in the Raman spectrum of graphitic carbon-based materials are the G and D peaks and their overtones. The first-order G and D peaks, both arising from the vibrations of sp^2 carbon, appeared at around 1580 cm^{-1} and 1354 cm^{-1} , respectively. The G peak corresponds to the optical E_{2g} phonons at the Brillouin zone center resulting from the bond stretching of sp^2 carbon pairs in both, rings and chains. The D peak represents the breathing mode of aromatic rings arising due to the defect in the sample [15]. The shift and shape of the overtone of the D peak, called as 2D peak around 2714 cm^{-1} , the 2D peak is attributed to double resonance transitions resulting in the production of two phonons with opposite momentum. Further, unlike the D peak, which is Raman active only in presence of defects, the 2D peak is active even in the absence of any defects. A defect-activated peak called D + G is also readily visible near 2900 cm^{-1} . The domain size was calculated using the Tuinstra and Koenig relation [16].

$$L_a = \frac{I_G}{I_D} C\lambda \quad (4)$$

where $C\lambda = C (514.5 \text{ nm}) \approx 4.4 \text{ nm}$ (C is the pre-factor) and L_a is the domain size. The intensity of the D and G peaks were estimated by fitting the spectrum. The film had a domain size of 5.13 nm . The intensity ratio of D band to G band, namely the I_D/I_G ratio, provides the gauge for the amount of structural defects, our graphene powder was found to have an I_D/I_G ratio of 0.8443 this value agreement with previous research [7,9,12].

4.2. Morphological properties

Atomic force microscope is a significant tool for the characterization of the surface morphology. Fig. 5 shows a typical three and two dimensional AFM image of graphene powder prepared by electrochemical exfoliation method with grain size equal to 86.89 nm and average surface roughness is 0.336 nm , its small amount due to effect of heat treatment during graphene powder drying. AFM showed the presence of irregularly shaped graphene sheets of non-uniform thicknesses having lateral dimensions ranging to a few nanometers

The surface morphology of the graphene powder grown also was investigated using the SEM as shown in Fig. 6. We observe the non-uniform distribution of particles in size and shape as it will be confirmed by AFM images, could be described as a collection of high density 3D clusters with a few agglomerates over the surface with different shapes, heights and sizes revealing a crumpled and rippled structure which was the result of deformation upon the exfoliation and restacking processes.

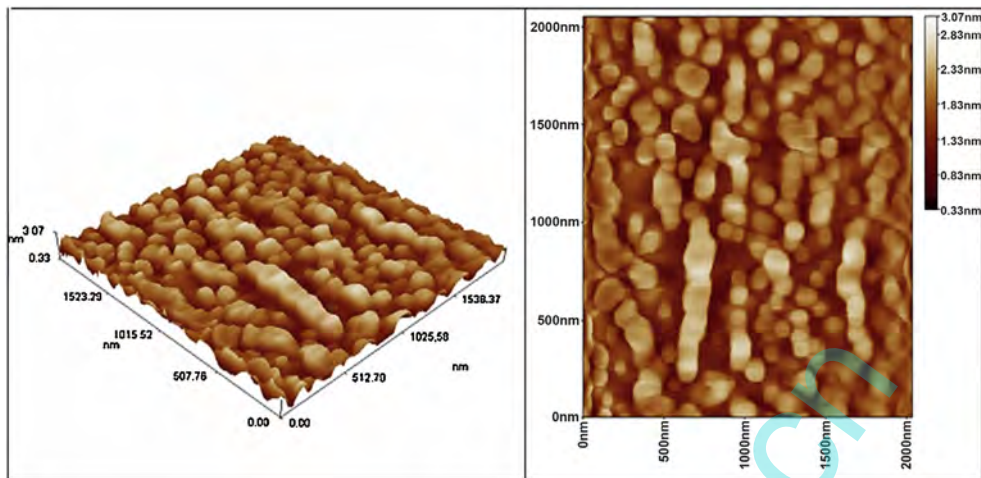


Fig. 5. 3-D and 2-D AFM image for graphene powder.

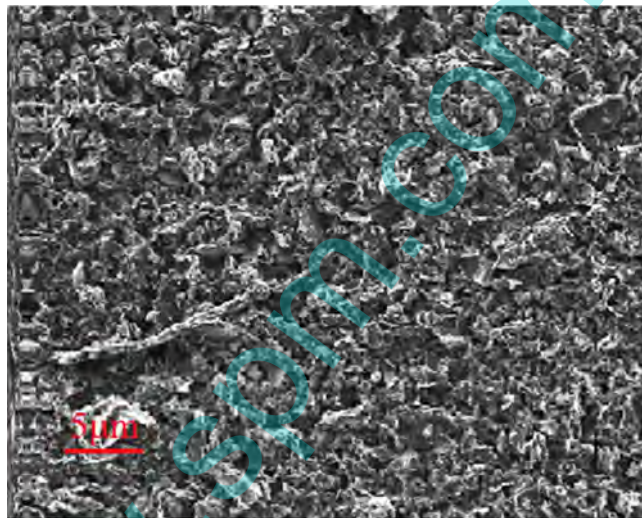


Fig. 6. SEM image of graphene powder at scale bars = 5 μm .

4.3. Chemical properties

FTIR spectroscopy is presented as a non-destructive analytical tool to determine the chemical bonds between atoms in materials. Transmission FTIR spectrum of graphene in a range of $400\text{--}4000\text{ cm}^{-1}$ are shown in Fig. 7. There are two peaks at 2865.67 cm^{-1} and 2918.4 corresponding to stretching vibration of C–H bonds in the high frequency area together with a sharp peak at 1465.95 cm^{-1} corresponding to the bending vibration of C–H groups of water molecules adsorbed on graphene. While the presence of two absorption peaks observed in the medium frequency area at 1643.41 cm^{-1} and 1095.6 cm^{-1} can be attributed to the stretching vibration of C=C aromatic groups and C–O of carboxylic acid and carbonyl groups respectively. Finally, Fig. 7 shows a broad peak at 3446.91 cm^{-1} corresponding to the stretching vibration of O–H bonds. These results are consistent with those reported earlier by Leila et al. [14], Mohammad et al. [17], and Satish et al. [18]. The presence of this types of oxygen functionalities with graphene may be caused by incomplete of heat treatment process.

5. Conclusions

We reported the formation and characterization of graphene powder synthesized by electrochemical exfoliation of graphite, this method was easy, controllable, and single step process. The structural properties showed good crystalline quality for graphene determined by XRD and Raman spectroscopy. The morphological properties exhibited nanostructure of graphene powder with different sizes characterized by SEM and AFM. FTIR spectrum showed the presence of C=C bond

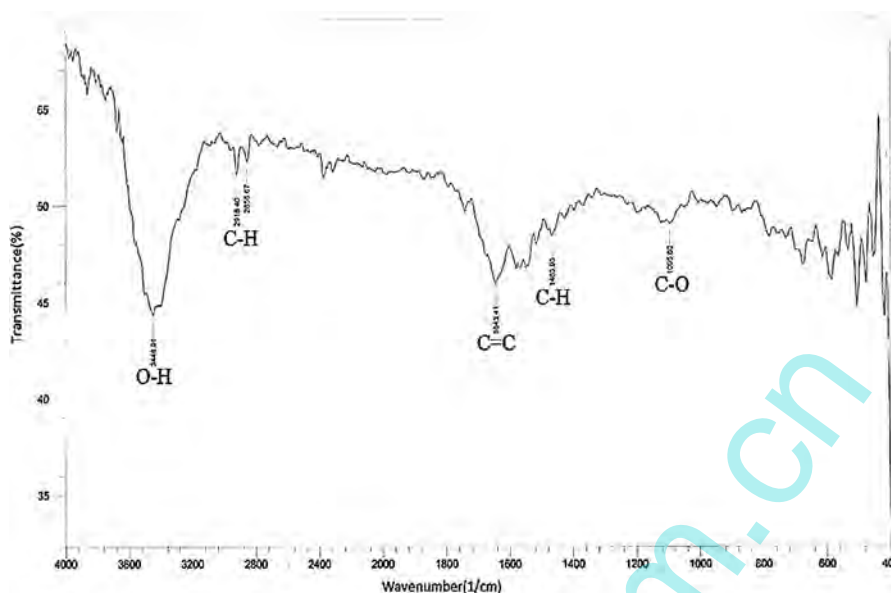


Fig. 7. FTIR transmittance spectrum of graphene as a function to wave number.

which indicates the formation of graphene, also presence of different types of oxygen functionalities with graphene such as C–O, and O–H bonds.

References

- [1] A. Dixit, D. Dixit, V.V. Chandrodaya, A. Kajla, Graphene: a new era of technology, *Int. J. Emerging Technol. Adv. Eng.* 3 (2013) 4–7.
- [2] Michael S. Fuhrer, Chun Ning Fuhrer, Allan H. MacDonald, Graphene materially better carbon, *MRS Bull.* 35 (2010) 289–295.
- [3] Mohammad Hakimi, Paransa Alimard, Graphene: synthesis and applications in biotechnology – a review, *World Appl. Program.* 2 (2012) 377–388.
- [4] A.K. Geim, Graphene: status and prospects, *Science* 324 (2009) 1530–1534.
- [5] M.I. Katsnelson, K.S. Novoselov, A.K. Geim, Chiral tunneling and the Klein paradox in graphene, *Nat. Phys.* 2 (2006) 620–625.
- [6] D.R. Dreyer, R.S. Ruoff, C.W. Bielawski, From conception to realization: an historical account of graphene and some perspectives for its future, *Angew. Chem. Int. Ed.* 49 (2010) 9336–9345.
- [7] C.T.J. Low, F.C. Walsh, M.H. Chakrabarti, M.A. Hashim, M.A. Hussain, Electrochemical approaches to the production of graphene flakes and their potential applications, *Carbon* 54 (2013) 1–21.
- [8] Hyunwoo Kim, Ahmed A. Abdala, Christopher W. Macosko, Graphene/Polymer nanocomposites, *Macromolecules* 43 (2010) 6515–6530.
- [9] Daniele Nuvoli, Valeria Alzari, Roberta Sanna, Sergio Scognamiglio, Massimo Piccinini, Laura Peponi, Josè Maria Kenny, Alberto Mariani, The production of concentrated dispersions of few-layer graphene by the direct exfoliation of graphite in organosilanes, *Nanoscale Res. Lett.* 674 (2012) 1–7.
- [10] Francesco Bonaccorso, Antonio Lombardo, Tawfique Hasan, Zhipei Sun, Luigi Colombo, Andrea C. Ferrari, Production and processing of graphene and 2d crystals, *Mater. Today* 15 (2012) 564–589.
- [11] Prashant Tripathi, Ch. Ravi Prakash Patel, M.A. Shazand, O.N. Srivastava, Synthesis of high-Quality graphene through electrochemical exfoliation of graphite in alkaline electrolyte, *RSC Adv.* 3 (2013) 11745–11750.
- [12] Ching-Yuan Su, Ang-Yu Lu, Yanping Xu, Fu-Rong Chen, Andrei N. Khlobystov, Lain-Jong Li, High-Quality thin graphene films from fast electrochemical exfoliation, *ACS Nano* 5 (2011) 2332–2339.
- [13] Seung Huh, Thermal reduction of graphene oxide, *Phys. Appl. Graphene Exp.* (2011) 73–90.
- [14] Leila Shahriary, Anjali A. Athawale, Graphene Oxide Synthesized by using Modified Hummers Approach, *Int. J. Renew. Energy Environ. Eng.* 2 (2014) 0157–2348.
- [15] F. Tuinstra, J.L. Koenig, Raman spectrum of graphite, *J. Chem. Phys.* 53 (1970) 1126–1130.
- [16] A.C. Ferrari, J. Robertson, Interpretation of Raman spectra, *Phys. Rev.* 61 (2000).
- [17] Mohammad A. Aldosari, Ali A. Othman, Edreese H. Alsharaeh, Synthesis and characterization of the in situ bulk polymerization of PMMA containing graphene sheets using microwave irradiation, *Molecules* 18 (2013) 3152–3167.
- [18] Satish Bykkam, Venkateswara Rao K, Shilpa Chakra CH, Tejaswi Thunugunta, Synthesis and characterization of ghrphene oxide and its antimicrobial activity against *Klebsiella* and *Staphylococcus*, *Int. J. Adv. Biotechnol. Res.* 4 (2013) 142–146.